Journal Name

ARTICLE

Cu(II) complexes of a tridentate N,N,O-donor Schiff base of pyridoxal: Synthesis, X-ray structures, DNA-binding properties and catecholase activity

Received 00th January 20xx,
Accepted 00th January 20xx

DOI: 10.1039/x0xx00000x

www.rsc.org/

Satyajit Mondal,[a] Moumita Chakraborty,[a] Antu Mondal,[a] Bholanath Pakhira,[a] Alexander J. Blake,[b] Ekkehard Sinn,[c] Shyamal Kumar Chattopadhyay*[a]

Two new Cu(II) complexes $[Cu(L_1)(N_3)]$(**1**) and $[Cu(L_1)(NCS)]_n$(**2**), where HL_1 ((E)-4-((2(dimethylamino)ethylimino)methyl)-5-(hydroxymethyl)-2-methylpyridin-3-ol) is a N,N,O-donor Schiff base ligand, have been synthesized. These complexes were characterized on the basis of spectroscopic, electrochemical, and other physicochemical properties. X-ray crystal structure determination reveals that in complex **1**, Cu(II) is in a square planar geometry with the N,N,O-donor ligand and a terminally coordinated azide ion. In complex **2**, however, Cu(II) assumes a square pyramidal geometry, and apart from the tridentate Schiff base ligand there is a thiocyanate ion, which acts in a $\mu_{1,3}$-bridging mode, connecting adjacent Cu(II) atoms in an axial-equatorial fashion forming an one dimensional chain. Cyclic voltammetry shows that complexes undergo Cu(II)/Cu(I) reductions at −0.40 to −0.55V followed by imine reduction at around −0.7V. Cu(I)/Cu(0) reduction is observed at approximately −0.9V. Complex **1** also shows appreciable catalytic activity for the aerial oxidation of 3,5 $DTBCH_2$ to DTBQ (catecholase activity). Both the complexes also show strong binding affinity towards calf-thymus DNA.

1. Introduction

Cu(II) ion plays an important role in biological systems and it is at the active site of various enzymes such as catechol oxidase, superoxide dismutase, multicopper oxidases.[1-8] Catechol oxidase is a copper-containing enzyme whose activity is similar to that of tyrosinase, a related class of copper oxidases. They are ubiquitous plant enzymes that catalyze oxidation of a broad range of *ortho*-diphenols to the corresponding *o*-quinones coupled with the reduction of oxygen to water. Krebs and co-workers reported the crystal structures of *deoxy* and *met* forms of catechol oxidase which reveal that these proteins have a dinuclear copper center.[1,9] The crystal structures of catechol oxidase have enhanced the understanding of the mechanism of catecholase activity of tyrosinase and/or catechol oxidase. Mechanisms of catechol oxidation by the neutral enzyme or synthetic model complexes have been proposed by various workers, prominent among them are the catalytic cycles proposed by Solomon and Krebs.[1,4,10,11] Model complexes have played an important role in understanding the structural, spectroscopic and catalytic properties of the copper sites in protiens.[12-26] Various workers have tried to rationalize the catalytic efficiency of the catechol oxidation reaction with variety of parameters like redox potentials, solvent effect, pH of the medium, number and nature of bridging ligands, effect of secondary coordination sphere etc., however our knowledge in this direction is still sketchy and incomplete.[12,13,17-26] Therefore, there is need for study of new model complexes showing catecholase activity and exploration of relationship between their structural, spectroscopic and catalytic properties.

From biological point of view, study of the Schiff bases of pyridoxal and their metal complexes are attractive for multiple reasons: pyridoxal is a close analogue of pyridoxine (vitamin B6) and thus its complexes may be bio-tolerable,[27] the manganese(II) complex of dipyridoxal diphosphate (N,N′-dipyridoxylethylenediamine-N,N′-diaceticacid 5,5′-bis(phosphate)) is a contrast agent for magnetic resonance imaging of the liver,[28,29] Cu(II) complex of pyridoxal has proven to be a highly promising candidate for the treatment of diabetic complications,[30] and so on. Therefore, we though it will be meaningful to synthesize pyridoxal appended ligands and to explore catalytic and biological properties of metal complexes of such ligands.[26,31]

Pseudohalide ions such as (N_3^-, NCS^-, NCO^-, and $N(NC)_2^-$) are versatile ligands that can bind transition metal ions in different of ways. They can behave as monodentate or as bridging ligands leading to the formation of mononuclear and polynuclear species. Among these, the azide and thiocyanate containing metal complexes are the most investigated systems because of their diverse structures and applications in magnetic materials.[32-34] The azide anion can bind to the metal ion through end on (EO) bridging mode, generally leading to ferromagnetic coupling, while the end to end (EE) bridging results in antiferromagnetic coupling. Furthermore, EE and EO bridging modes may simultaneously exist in some species, leading to different topologies and materials with unprecedented, magnetic behaviour.[35-37] On the other hand SCN^- anion is a highly versatile ambidentate ligand with two donor atoms. It can coordinate either through the N or the S atom, or both, giving rise to linkage isomers,[38,39] dimers[40] or polymers.[41]

The interaction of small molecules with DNA has been an active area of research at the interface of chemistry and biology.[42-47] These small molecules are stabilized on binding to DNA through a series of weak interactions, such as the π-stacking interactions associated with intercalation of a planar aromatic group between the base pairs, hydrogen-bonding and van der Waals interactions of functionalities bound along the groove of the DNA helix,[48] and the electrostatic interaction of the cation with phosphate group of DNA.[49] In recent years there is significant upsurge in the study of binding of transition metal complexes to DNA, with the aim of developing new DNA foot printing and DNA cleaving agents as well as identifying potential anticancer drugs.[50-54]

In this paper, we describe, the syntheses of two Cu(II) complexes $[Cu(L_1)(N_3)]$(**1**) and $[Cu(L_1)(NCS)]_n$ (**2**), of a N,N,O-donor pyridoxal Schiff

[a] Department of Chemistry, Indian Institute of Engineering Science and Technology, Shibpur, Howrah 711103, India. shch20@hotmail.com (S.K. Chattopadhyay).
[b] School of Chemistry, The University of Nottingham, University Park, Nottingham, Nottinghamshire, NG7 2RD, UK.
[c] Chemistry Department, Western Michigan University, Kalamazoo, MI 49008-5413, USA
† Electronic Supplementary Information (ESI) available:
See DOI: 10.1039/x0xx00000x

base ligand (HL_1). Their single crystal X-ray structures have been determined. The spectroscopic and electrochemical properties of the complexes were investigated. DNA binding affinity of these complexes was also studied. 3,5-DTBC was used as a model substrate to study the catecholase activity of the complexes and only **1** was found to be catalytically active.

2. Experimental

2.1 Materials and methods

Pyridoxal hydrochloride was purchased from Aldrich and triethylenetetramine was purchased from E. Merck. All other chemicals and solvents were of reagent grade and used as such. Solvents for spectroscopic and cyclic voltammetry studies were of HPLC grade obtained from Merck or Aldrich. Elemental analyses were performed on a Perkin–Elmer 2400 C, H, N analyzer. Infrared spectra were recorded as KBr pellets on a JASCO FT-IR-460 spectrophotometer. UV–Vis spectra were recorded using a JASCO V-630 spectrophotometer. ^{1}H NMR spectra were recorded on a Bruker AVANCE DPX 300 MHz spectrometer using, $Si(CH_3)_4$ as internal standard. ESI-MS spectra of the samples were recorded on JEOL JMS 600 instrument. Fluorescence spectra at room temperature were recorded using PTI made QuantaMaster40 spectro-fluoremeter. EPR spectrum of complex **2** was recorded in DMF solution at 77K with a Varian E-112 EPR Spectrometer at SAIF, IIT, Bombay.

2.2 Synthesis of Ligand (HL_1)

Pyridoxal hydrochloride (0.203 g, 1mmol) was dissolved in 40 mL methanol and the pH was set to 6.5-7.0 by addition of concentrated aqueous KOH solution. On dropwise addition of methanolic N,N-dimethylethylenediamine (0.088 g, 1mmol) to the neutral pyridoxal solution, the reaction mixture turned light yellow with no formation of precipitate. The solution was refluxed for three hours and then the solvent was evaporated on a rotary evaporator, when a yellowish brown oily product was obtained. It was triturated with acetone and then recrystallized from methanol to give a yellow hygroscopic solid. The ligand was characterized by analytical, spectral (IR, NMR, UV-vis, Emission, ESI-MS) and electrochemical studies. Yield: 205 mg (86%). Anal.calc.for $C_{12}H_{19}N_3O_2$ (MW 237.15): C, 60.74; H, 8.07; N, 17.71. Found: C, 60.44; H, 8.26; N, 17.91%. ESI-MS: m/z: 238.04 $[(L+H])^+$ (100) % (**Figure S1** in the Supporting Information, SI). ^{1}H-NMR (DMSO-d6): δ(ppm): 8.75(1H, s), 7.8(1H, s), 4.5 (2H, s), 2.8(2H, d), 2.7-2.6(2H, t), 2.5(3H, s), 2.1(3H, s), 1.94(3H, s) (**Figure S2** in the SI). ^{13}C-NMR(DMSO-d6): δ(ppm): 134.88, 133.31, 132.1, 129.13, 70.60, 67.85, 59.09, 30.23, 28.80, 22.85, 14.36, 11.260 (**Figure S3** in the SI). Electronic spectrum in (0.01 M Tris-HCl buffer, pH 7.4): λ_{max}/nm(ε_{max} /$M^{-1}cm^{-1}$): 416 (sh, 1640), 333(8321), 287(9272), 250(12290). Selected IR bands (cm^{-1}): 3406 br(ν_{O-H}), 3042 (ν_{N-H}), 1628 ($\nu_{C=N}$) (**Figure S4** in the SI).

2.3. Synthesis of the complexes

A methanolic solution (5 ml) of the ligand HL_1 (0.206 g, 1 mmol) was added dropwise to a solution of $Cu(ClO_4)_2{\cdot}6H_2O$ (0.370 g, 1 mmol) in the same solvent (5 ml). After the mixture was refluxed for 1 h, an aqueous solution of NaN_3 (0.130 g, 2 mmol) or KSCN (0.194 g, 2 mmol) was added, and the resulting mixture was refluxed for further 3 h. The green solution was filtered and the supernatant liquid was kept at room temperature for slow evaporation. After one day, green crystals of $[Cu(L_1)(N_3)]$ (**1**) or $[Cu(L_1)(SCN)]_n$ (**2**), suitable for X-ray structure determination were obtained.

For $[Cu(L_1)(N_3)]$(1)

Yield: 270 mg (79%). Anal. calc. for $C_{12}H_{18}CuN_6O_2$ (M.W. 341·86):C, 42.12; H, 5.26; N, 24.6. Found: C, 42.26; H, 5.30; N, 24.4%. MS: m/z: 299.09 $[CuL_1]^+$(100%)] (**Figure S5** in SI). Electronic spectrum in CH_3OH solution λ_{max}/nm(ε_{max}/$M^{-1}cm^{-1}$): 613(163), 384(3970) 270(7108), 228(13467). Selected IR bands (cm^{-1}): 3398br(ν_{OH}), 2930(ν_{CH}), 2057(ν_{N3}), 1641($\nu_{C=N}$), 1422($\nu_{C-O\ phenol}$).

For $[Cu(L_1)(NCS)]_n$(2)

Yield: 290 mg (80%). Anal. calc. for $C_{12}H_{18}CuN_4O_3S$ (M.W. 359.91): C, 39.8; H, 4.97; N, 15.5. Found: C, 39.35; H, 4.85; N, 15.34%. MS: m/z: 301.15 $[CuL_1H]^+$(100%)] (**Figure S6** in SI). Electronic spectrum in CH_3OH solution λ_{max}/nm(ε_{max}/$M^{-1}cm^{-1}$): 634(142), 388(3902), 270(7416), 223(14448). Selected IR bands (cm^{-1}): 3232br(ν_{OH}), 2095(ν_{SCN}), 1628($\nu_{C=N}$), 1417($\nu_{C-O\ phenol}$).

Table 1: Crystal data and refinement details of **1** and **2**.

Compounds	1	2
Formula	$C_{12}H_{18}CuN_6O_2$	$C_{12}H_{18}CuN_4O_3S$
Formula weight	341.86	359.91
Crystal size(mm)	0.393×0.194×0.151	0.20×0.18×0.105
Temperature (K)	150(2)	100(2)
Crystal system	Monoclinic	Monoclinic
Space group	P 2_1/c	P 2_1/n
a (Å)	6.7493(17)	11.2788(4)
b (Å)	11.511(3)	10.1456(4)
c(Å)	17.901(5)	14.1768(5)
α(°)	90	90
β(°)	94.172(11)	112.976(2)
γ(°)	90	90
dcal	1.637	1.592
μ(mm−1)	1.590	1.611
F(000)	708	740
Total Reflections	3398	3564
Observed data [I>2σ(I)]	2407	2594
R1, wR2 [I>2σ(I)]	0.0573, 0.0997	0.0479, 0.0997
R1, wR2 (all data)	0.0991, 0.1269	0.0851, 0.1151
Data/restraints/parameters	3398/0/206	3564/0/197
Goodness-of-fit (GOF) on F2	1.053	1.057

2.4 X-ray crystallography

X-ray diffraction data for **1** was collected on a Agilent GV1000 Atlas diffractometer at 150(2)K using Cu-Kα radiation (λ= 1.54184 Å). Data collection and reduction were done using CrysalisPro program[55] and empirical absorption correction using spherical harmonics, were implemented in Scale3 Abspack Scaling Algorithm within CrysalisPro. Structure was solved by Direct method using SHELXS 97 and refined by full-matrix least-squares on F^2 using SHELEXL version 2014/3.[56,57] X-ray diffraction data for **2** was collected on a Bruker SMART APEX II diffractometer at 100 (2) K, utilizing a graphite monochromated Mo-Kα radiation (λ= 0.71073 Å). Data was indexed and refined as a nonmerohedral twin with two domains using Bruker SAINT V8.18C program.[58] The ratio between the domains is 0.190(5). Structure was solved by Direct method using SHELXS-97 and refined by full-matrix least-squares on F^2 using SHELEXL version 2017/1.[56,57] Data were corrected for absorption effects using the Bruker 'TWINABS' program.[59] The non-hydrogen atoms were refined with anisotropic displacement parameters. All hydrogen atoms were placed at calculated positions and refined as riding atoms using

isotropic displacement parameters. A summary of the crystallographic data is presented in **Table 1**. Important bond distances and bond angles are collected in **Table 2**. Crystal data have been deposited at CCDC with deposition numbers 1817674 and 1817791 for and **1** and **2** respectively.

2.5. DNA-binding experiments

2.5.1. Absorption spectral studies

The DNA binding experiments were performed in Tris–HCl/NaCl buffer (50 mM Tris–HCl/1 mM NaCl buffer, pH 7.3) using a methanol (CH_3OH) solution of complexes **1** and **2**. The concentration of CT-DNA was determined from the absorption intensity at 260 nm with a ε value of 6600 $M^{-1}cm^{-1}$.[60] The UV absorbance ratio at 260 and 280 nm (A_{260}/A_{280}) of 1.85 indicated that the DNA was sufficiently free of protein contamination.[61] The DNA stock solution was stored at 4°C in the dark and used within 4 days after preparation. The concentrated stock solutions of complexes **1** and **2** were prepared by dissolving them in CH_3OH and diluting suitably with Tris–HCl (pH 7.4) buffer. Complex-DNA solutions were allowed to incubate for 5 min before the absorption spectra were recorded. The intrinsic binding constant K_b was calculated from the spectroscopic titration data using the following equation:[62]

$$[DNA]/(\varepsilon_a - \varepsilon_f) = [DNA]/(\varepsilon_b - \varepsilon_f) + 1/K_b(\varepsilon_b - \varepsilon_f) \quad .....(1)$$

where ε_f and ε_b are the extinction coefficients of the free and fully bound complex while ε_a is the extinction coefficient observed for the absorption band at a given DNA concentration, K_b the equilibrium binding constant. A plot of $[DNA]/(\varepsilon_a - \varepsilon_f)$ versus [DNA] gives K_b as the ratio of the slope to the intercept.

2.5.2. Fluorescence spectral studies

For fluorescence quenching experiments DNA was pretreated with ethidium bromide and kept in at 4°C for 4 hour. The complexes were then added to this mixture and their effect on the emission intensity was measured using PTI made QuantaMaster40 spectro-fluoremeter. Samples were excited at 520 nm and emission was observed between 540 to 700 nm.

2.6. Electrochemical studies

Electrochemical data of 1-2 mM DMF solutions of the complexes were collected using a CH1106A potentiostat. A three electrode configuration, consisting of a glassy carbon working electrode and a Pt-wire auxiliary electrode, TEAP as supporting electrolyte and Ag,AgCl/KCl reference electrode, with scan rate rate (20-100) Vs^{-1} was used. The potentials were calibrated against the ferrocene/ferrocenium couple (E_0 = 0.44 V). Electrochemical titrations of copper complexes with CT-DNA were recorded by cyclic voltammetry and DPV in DMF solutions at room temperature.

2.7 Catalytic activity for the oxidation of 3,5-di-tert-butylcatechol

The catalytic oxidation of substrate 3,5-di-tert-butylcatechol ($DTBCH_2$) by [Cu(L)(N_3)] (**1**) complex was performed in methanol at room temperature. The reaction was carried out spectrophotometrically by monitoring the increase in the absorbance band of 3,5-di-tert-butyl-1,2-benzoquinone (3,5-DTBQ) at 400 nm as a function of time. Absorbance vs. wavelength plots were recorded for these solutions at a regular time interval of 5 min in the range 300–500 nm. The minimum and maximum complex to substrate ratio was 1:16 and 1:500 respectively. Km, V_{max} and k_{cat} values were determined by Lineweaver–Burk plots and Michaelis–Menten equation.

2.8 Detection of Hydrogen Peroxide in the Catalytic Reaction

The presence of hydrogen peroxide in the reaction mixture was analyzed iodometrically by assaying I_3^-, which has a characteristic absorption band at 353 nm (ε = 26000 $M^{-1}cm^{-1}$ in water). The oxidation reaction of $DTBCH_2$ by complex **1** was carried out as described in the kinetic experiment. When the formation of quinone reached a desired value at 400 nm the solution was acidified with H_2SO_4 to pH 2 to stop the reaction. Water (3 ml) was added and the reaction mixture was then extracted two times with CH_2Cl_2 to remove the DTBQ formed during the reaction. To a 2 ml aliquot of the aqueous layer 1 ml of a KI solution (0.3 M) was added with a catalytic amount of ammonium molybdate (3% solution) to accelerate the formation of I_3^-. Blank experiments were performed under identical conditions in the presence of DTBQ and complex **1**, but only minor formation of $I_3^-$was observed.

2.9 DFT

In order to understand the electronic structure of the synthesized complex **1** and **2**, we have carried out DFT calculations with the Gaussian 03 package (revision B.04).[63] Molecular orbitals were visualized using Gauss View. Single point calculations, and population analysis of the molecular orbitals were carried out using the density functional theory (DFT) with B3LYP hybrid exchange functional.[64,65] For H, C, N and O atoms 6-31G* basis set were used.[66] The LANL2DZ basis set[67] and LANL2DZ pseudopotentials of Hay and Wadt[68] were used for the Cu atom. The geometry of the complexes was taken from the crystal structure, and single point energy calculated, without further optimization, in gas phase.

3. Results and discussion

3.1 Synthesis of complexes

The Cu(II) complexes **1** and **2** were synthesized by refluxing a mixture of methanolic solution of $Cu(ClO_4)_2{\cdot}6H_2O$ and aqueous solution of pseudo halides (NaN_3, KSCN) with the ligand. After filtration, on slow evaporation of the filtrate at room temperature, green colored square shaped crystals of the complexes suitable for X-ray diffraction studies, appeared after 1 day. A simple scheme showing the synthesis of complex is depicted in **Scheme I**. The isolated complexes were characterized by elemental analysis, IR, UV–vis spectroscopy, CV, and by single-crystal X-ray crystallography.

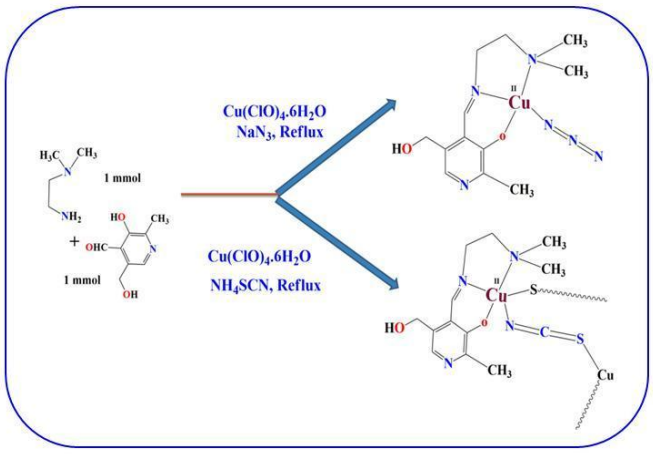

Scheme I: Schematic representation of the synthesis of the Metal complexes.

3.2 Description of X-ray crystal structure

The ORTEP diagrams along with atom numbering scheme for complexes **1** and **2** are shown in **Figures 1** and **2** respectively and the important bond lengths and angles are listed in **Table 2**. In the complex **1**, the copper ion

occupies the central position of a regular square planar arrangement. Out of its four coordination sites three are occupied by the phenolato oxygen, imine nitrogen, and the tertiary amine nitrogen of the tridentate ligand. The remaining fourth coordination site is satisfied by an azido group which is linked to Cu(II) ion through a terminal nitrogen atom. The azide group, which acts as a monodentate ligand is slightly asymmetric [N(4)–N(5)=1.184(2) and N(5)–N(6)=1.163(2)Å] and linear within the experimental error [N(6)–N(5)–N(4)=177.1(2)°]. The structure of **1**, however, differs from few other X-ray crystallographically investigated Cu(II) azide complexes containing terminal azido ligand.[69,70] In most of the Cu(II) complexes having a terminal azide ligand the coordination geometry around copper ion is either pseudo octahedral or distorted trigonal bipyramidal, while square planar arrangement, as observed in complex **1**, is not so common.

In complex **2**, however, Cu(II) assumes a square pyramidal geometry (τ = 0.18; τ = 0 for square pyramid and 1 for trigonal bipyramid). The N,N,O-donor atoms of the tridentate ligand along with a thiocyanate N occupies the square plane, and the axial position is occupied by a thiocyanate sulfur atom of an adjacent unit at ½ – x, ½ + y, ½ – z. The thiocyanate ion thus acts as a $\mu_{1,3}$–bridge connecting adjacent Cu(II) atoms in an axial– equatorial fashion, forming an one-dimensional chain along 'b' axis (**Figure S 7**).

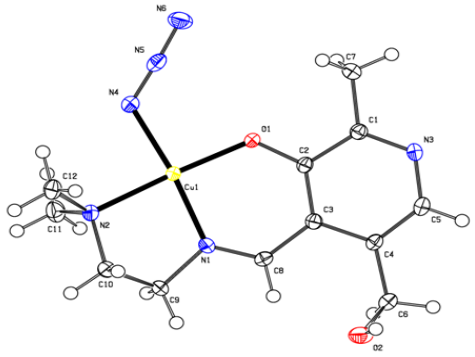

Figure 1 ORTEP diagram (50% probability level) for **1**.

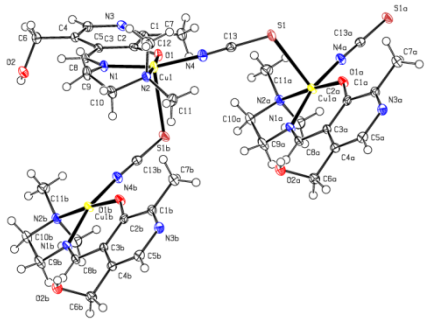

Figure 2 ORTEP diagram (50% probability level) for **2**.

Table 2 Selected bond distances (Å) & bond angles (⁰) for **1** and **2**.

1			
Bond lengths [Å]		Bond angles [°]	
Cu1–N1	1.9313(16)	N1–Cu1–N2	84.72(7)
Cu1–N2	2.0627(16)	N1–Cu1–N4	169.23(7)
Cu1–N4	1.9591(17)	N2–Cu1–N4	90.17(7)
Cu1–O1	1.9088(13)	O1–Cu1–N1	93.07(6)
		O1–Cu1–N2	173.78(6)
		O1–Cu1–N4	92.94(7)
2			
Cu1– N1	1.949(3)	N1– Cu1– N2	84.23(12)
Cu1– N2	2.045(3)	N1– Cu1– N4	164.54(13)
Cu1– N4	1.972(3)	N2– Cu1– N4	92.06(12)
Cu1– O1	1.900(3)	O1– Cu1– N1	92.84(11)
Cu1– S1b	2.836(1)	O1– Cu1– N2	175.33(10)
		O1– Cu1– N4	89.82(11)

Symmetry code b = ½ – x, ½ + y, ½ – z

3.3 Infrared spectra

In the complexes bands appearing at 3402 and 3228 cm^{-1} are assigned to the O–H stretching vibrations of coordinated hydroxymethyl group and bands at 2928 and 2920 cm^{-1} indicate the presence of aromatic C–H stretching vibration of pyridine moiety. The band corresponding to the C=N stretching vibration appears at 1629 cm^{-1} in the ligand, which shifts to higher wavelength at 1644 cm^{-1} in the complexes indicating imine nitrogen is coordinated to metal atom. Complex **1** shows strong sharp absorption band at 2062 cm^{-1} corresponds to the asymmetric stretching mode of monodentate azide ligand (**Figure S8**). Free azide ion in NaN_3 shows single strong absorption centred at 2133 cm^{-1}.[71] The shift to lower wave numbers indicates the coordination of azide ion to Cu(II) in the complex. Potassium thiocyanate shows a very strong band at 2048 cm^{-1} in i.r spectrum, which is caused by the C≡N stretching vibration. However, in complex **2** this band is shifted to higher frequency at ~2100 cm^{-1} suggesting coordination of the thiocyanate group to the metal centre (**Figure S8**).

3.4 Electronic spectra

The absorption spectra of the ligand (HL_1), and the complexes **1** and **2**, were recorded at a concentration of 10^{-4} M in CH_3OH, as the complexes show good solubility in CH_3OH. The spectrum of the ligand exhibits two absorption bands at 287 and 333 nm attributable to the π→ π* transition associated with the azomethine chromophore and n→π* transitions involving the phenolic oxygen respectively. In the case of the complexes **1** and **2**, the n→π* transition was shifted to a much greater extent, from 333 to 384 or 388 nm; this indicates the phenolic oxygen had lost a hydrogen on coordination to the metal centre. The broad transition around 615 and 634 nm for complexes **1** and **2** respectively corresponds to a d-d transition of the Cu(II) centre (**Figure 3**).[72]

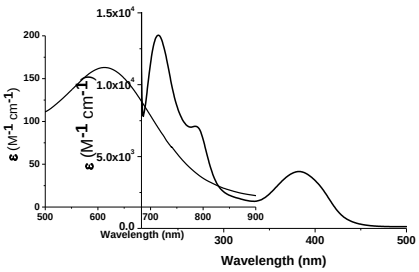

Figure 3 Electronic spectra of the complexes **1 (a and b)** and **2 (c and d)**.

3.5 Cyclic voltammetry studies:

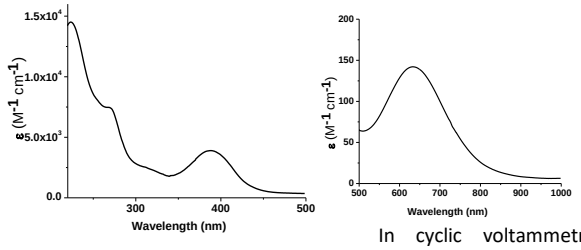

In cyclic voltammetry (CV) experiments, on the negative side of the reference electrode, complex **1** shows two overlapping reductive peaks at −0.66 V and −0.87 V. On scan reversal a broad

anodic wave spanning −0.4 to −0.6 V was observed (**Figure 4**). In the differential pulse voltammetry (DPV) two well resolved peaks at −0.55 V and −0.68 V were observed. The tail of the second reductive wave extends beyond −1.0 V, but no peak could be resolved between −0.8 to −1.0 V. We believe the CV peak at −0.66 V corresponds to DPV peaks at −0.55 V and −0.68 V and they denote Cu(II)/Cu(I) and imine reductions respectively (note that β-LUMO is predominantly metal centered while α-LUMO has appreciable contribution from imine part of the ligand, *vide infra*). The Zn(II) complex of the ligand shows a reductive DPV peaks at −0.66 V and this supports the above assignment (**Figure S9**). The CV peak at −0.87 V probably corresponds to Cu(I)/Cu(0) reduction, which is buried under the tail of the ligand reduction peak in DPV.

In the case of complex **2** in CV, a quasi-reversible reductive wave at −0.42 V (ΔE_p = 190 mV) is followed by a near irreversible reductive peak at −0.87 V. In DPV, again three well resolved peaks are observed at −0.43, −0.61 and −0.78 V. However, the last two peaks have current heights much smaller than the peak at −0.43 V. Following the discussion for complex **1**, we assigned the three peaks at −0.43, −0.61 and −0.78 V to Cu(II)/Cu(I), imine reduction and Cu(I)/Cu(0) processes respectively. Probably on reduction to Cu(I) the complex undergoes ligand dissociation in this case and this may explain the relatively smaller peak heights of the peaks at −0.61 and −0.78 V.

CV and DPV provide an additional and sensitive tool to study binding of metal complexes to DNA. On addition of DNA to complex 1, the DPV peaks shift towards less negative value. The difference in redox potential between the DNA-bound complex and the free complex is represented by following equation: E_b-E_f = 0.059 log(K_{red}/K_{ox}), where K_{red} and K_{ox} are, respectively, stability constants of the binding of the oxidized (K_{ox}) or reduced forms (K_{red}) with DNA and E_b and E_f are redox potentials in bound and free forms of the complex. The positive value of E_b-E_f (0.06V) for complex **1** indicates that the reduced complex binds to the DNA approximately ten times stronger than the oxidized form**.**

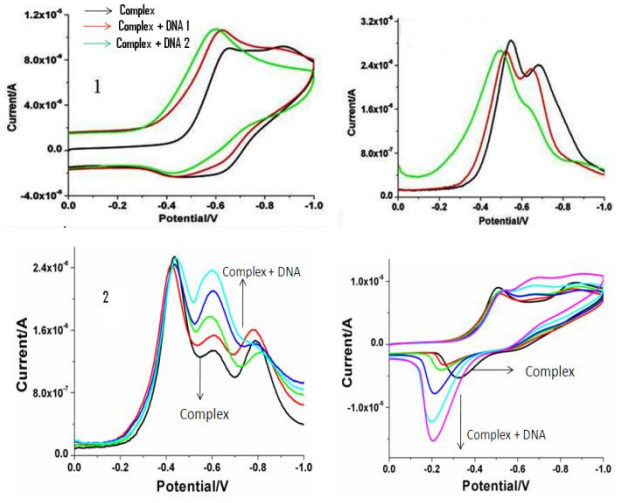

Figure 4 CV and DPV of complex **1** and **2** in DMF solution upon addition of DNA (DNA 1 and DNA2 refers to increasing amount of DNA), at a GC electrode at 100 mV s^{-1} scan rate.

Unlike complex **1**, addition of DNA to complex **2** does not change the peak positions of DPV much, indicating the oxidized and reduced complexes have very similar affinity for DNA.

3.6 EPR spectra

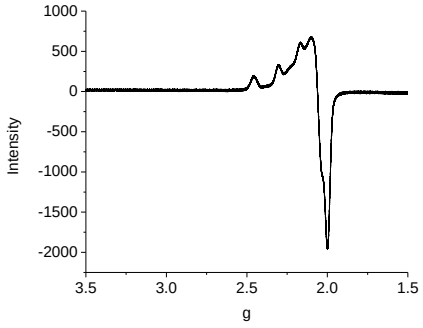

Figure 5 X-band EPR spectrum of complex **2** in DMF glass at 77K.

EPR spectra is an important tool to study the electronic and geometrical features of Cu(II) complexes. We have recorded the epr spectrum of complex **2**, as a representative example, in DMF solution at 77K (**Figure 5**). The complex shows typical axial spectra expected of a 4+1 coordinated complex with $g_{\|}$ (2.23) > $g_{\perp}$ (2.05), and $A_{\|}$ = 168 × 10^{-4} cm^{-1}, indicating the unpaired electron is in d_{x2-y2} orbital.

3.7 DNA binding study

3.7.1 Absorption spectroscopic studies

The interaction of variety of small molecules (metal complexes) with DNA double helix occurs by three distinct binding modes. They are, (i) Electrostatic binding / External binding: Complexes are positively charged and the DNA phosphate sugar backbone is negatively charged and their interaction is known as electrostatic. (ii) Groove binding: The molecules approach within van der Waals contact and reside in the DNA groove. Hydrophobic and/or hydrogen-

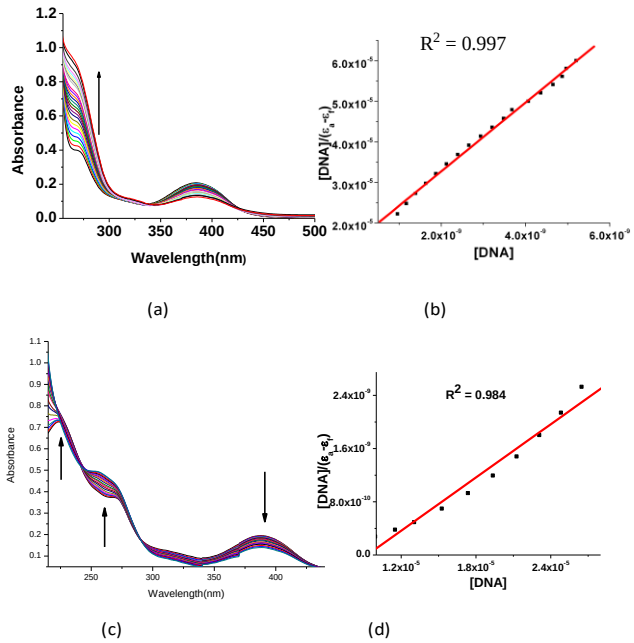

Figure 6 Absorption spectra of complexes **1** (a) and **2** (c) (1.0 × 10^{-4}, 5.0 × 10^{-5} M respectively) in the presence of increasing amounts of CT-DNA (3.0 × 10^{-4}, 1.0 × 10^{-4} M) at room temperature in 5 mM Tris-HCl/NaCl buffer (pH = 7.4) at 25°C. The arrow shows the absorbance changing upon increasing the DNA concentration. The plots of [DNA]/εa – εf) versus [DNA] for the titration of DNA with the Cu(II) complexes are shown in (b) and (d).

bonding are usually important components of this binding process, and provide stabilization. (iii) Intercalative binding / Intercalation: this association involves the insertion of planar fused aromatic ring system between the DNA base pairs, leading to significant π- electron overlap. The study of the binding capacity of the metal complexes to DNA double helix may be studied by electronic absorption spectroscopy, which follows the changes in the absorbance and shift in wavelength (**Figure 6**). The variation of absorption spectra with the addition of CT-DNA to the solution of the complexes was followed. It was seen that on binding of DNA by the complexes, the UV absorbance at ~270 nm increases, this absorbance increase is referred to as a "hyperchromic shift" or the hyperchromic effect. The characteristic feature of hyperchromic shift is the extent of increase of the absorbance of the ligand centered band.[73] With increase of concentration of CT- DNA, both the complexes showed a hyperchromic and a slight blue-shifted LC band in the absorption spectra. The hyperchromic values observed in the presence of DNA were in the range 17.4–57.2%, and their blue shifts are by 3-4 nm (Table 3). The intrinsic binding constant K_b calculated from the plots of [DNA]/(ε_a- ε_f) verses [DNA] can be obtained from the ratio of the slope to the intercept. Using the hyperchromism at 266 and 270 nm the intrinsic binding constant K_b for DNA binding by the complexes **1** and **2** were determined to be 5.4 × 10^8 and 1.08 × 10^5 M^{-1} respectively. The exceptionally high value of K_b for **1**, which is relatively higher than the classical intercalator (ethidium bromide; 1.4 × 10^6 M^{-1}), suggests the complex is an avid binder of DNA. Since such high binding constant is generally characteristic of DNA binding by intercalation, so we assume that the complexes **1** and **2** bind DNA predominantly by intercalation, though H-bonding, electrostatic interactions as well as interactions with the phosphate groups of DNA may also lend their contribution towards overall binding strength.

Table 3: Electronic absorption spectral properties of the complexes on DNA binding.

Complex	λ_{max}(nm)	λ_{max}(nm)	Δλ(nm)	%H[a]	[b]K_b(M^{-1})	[b]K_{SV} (M^{-1})	[c]Kapp (M^{-1})
	Free	Bound					
1	270	266	4	57.2	5.39 × 10^8	1.67 × 10^5	1.07 × 10^7
2	270	267	3	17.4	1.08 × 10^5	2.12 × 10^5	2.46 × 10^6

[a]H% = [(A_{bound} - A_{free}) /A_{bound}] × 100%; [b]K_b = Intrinsic DNA binding constant determined from the UV - Vis absorption spectral titration, [c]K_{SV} and [c]K_{app} are Stern-Volmer constant and apparent binding constant obtained from fluorescence spectrsocopy

3.7.2 Fluorescence binding study

Ethidium bromide is a planar cationic dye which is widely used as a sensitive fluorescence probe for native DNA. Its fluorescence intensity is very weak, but it is greatly increased when EB is specifically intercalated into the base pairs of DNA.[74,75] Furthermore, this fluorescence is quenched by the addition of another molecule that displaces EB from DNA.[54] It was found that the fluorescence intensity of CT-DNA-EB decreased remarkably with the addition of the complexes **1** and **2** (**Figure 7**), which indicated that the complexes can bind DNA and replace EB from the CT-DNA-EB system.[76] The fluorescence quenching data can be fitted with Stern Volmer equation:[77] I^0/I = 1 +Ksv[Q], where Ksv is the quenching constant, and [Q] is the quencher concentration. In the linear fit plot of I^0/I versus [complex], Ksv is given by the slope of the plot. The Ksv values for the complexes **1** and **2** were determined to be 1.67 × 10^5M^{-1} (R^2 = 0.990) and 2.12 × 10^5M^{-1} (R = 0.990) (I^0 is the emission intensity of EB-DNA in the absence of complex; I is the emission intensity of EB-DNA in the presence of complex). The apparent binding constant (Kapp) was estimated at 1.07 × 10^7 M^{-1} for **1** and 2.46 × 10^6 M^{-1} for **2** (Table 3) using the equation K_{EB}[EB] = Kapp[complex], where the complex concentration was the value at a 50% reduction of fluorescence intensity of EB and K_{EB} is 1.0 × 10^7 M^{-1} and [EB] was taken as 5.0 × 10^{-6} M^{-1}.[78] The high Kapp value implies that the complexes **1** and **2** can strongly interact with DNA.

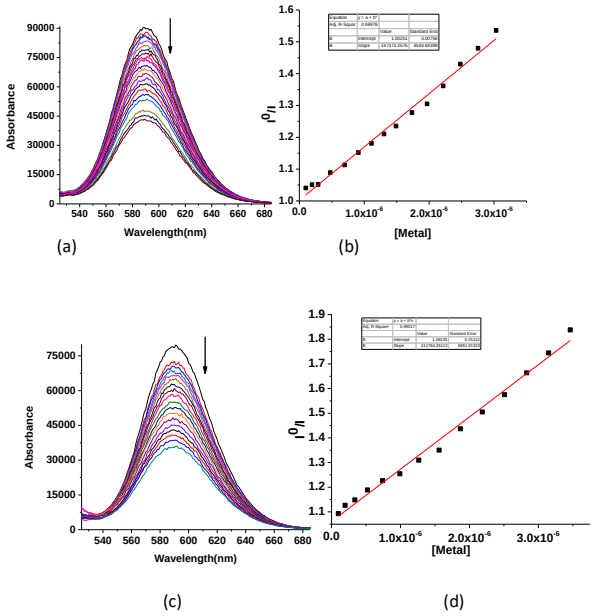

Figure 7 Fluorescence titration of Ethidium bromide-DNA complex with complex **1** (a) and **2**(c) and their Stern Volmer plots (b for complex **1** and d for complex **2**)

3.8 Catecholase activity of Complex 1

3.8.1 Kinetics of 3, 5-di-tert-butylcatechol oxidation

Kinetic experiments for the oxidation of $DTBCH_2$ (3,5-di-tertbutylcatechol) by [Cu(L)(N_3)](**1**) (**2** was ineffective as catalyst for catecholase reaction) was evaluated in methanol by monitoring the increase in absorbance at 400 nm as a function of time over the first 5 min corresponding to the formation of the quinone product DTBQ (3,5-di-tert-butyl-obenzoquinone). In a typical experiment, 2000 µl of a solution of **1** in methanol ($[C]_o$= 6 × 10^{-4} M) was added to a 1-cm-path-length cell containing 3 cm^3 of methanol at 25°C. The reaction was initiated by the addition of 100 µl of catechol solution ($[3, 5-DTBC]_o$= 2.0 × 10^{-3} to 6.0 ×10^{-2} M). A kinetic treatment on the basis of the Michaelis-Menten approach was applied and the various kinetic parameters V_{max}, K_M and k_{cat} were evaluated from Lineweaver-Burk double-reciprocal plots.[78] The observed rate versus [substrate] plot in methanol solution as well as Lineweaver–Burk plot are given in **Figure 8**. The kinetic parameters are listed in **Table 4**. The turnover number (k_{cat}) at 898 h^{-1} is reasonably good.

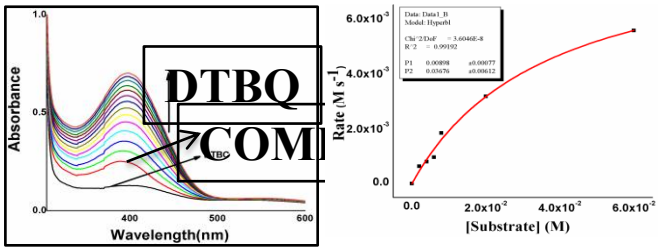

(a) (b)

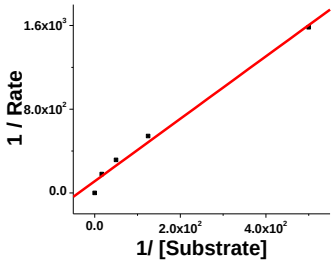

(c)

Figure 8 (a) The changes of UV–Vis spectral behavior at regular interval of time for complex **1** in methanol medium upon addition of 3,5-DTBC observed after each 5 min interval. (b) Plot of rate vs. substrate concentration for complex **1. (c)** Linweaver-Burk plot of complex **1**.

Table 4: Kinetics parameters for the oxidation of 3,5-DTBC catalyzed by Cu (II) complex (**1**).

Complex	$V_{max}(Ms^{-1})$	$K_m(M)$	R	$k_{cat}(h^{-1})$	K_{cat}/K_M $M^{-1}h^{-1}$
1	8.9×10^{-3}	0.036	0.992	898	2.49×10^4

3.8.2 Mechanistic aspects towards catalytic oxidation of 3,5-di-tert-butylcatechol (DTBC) by Complex 1

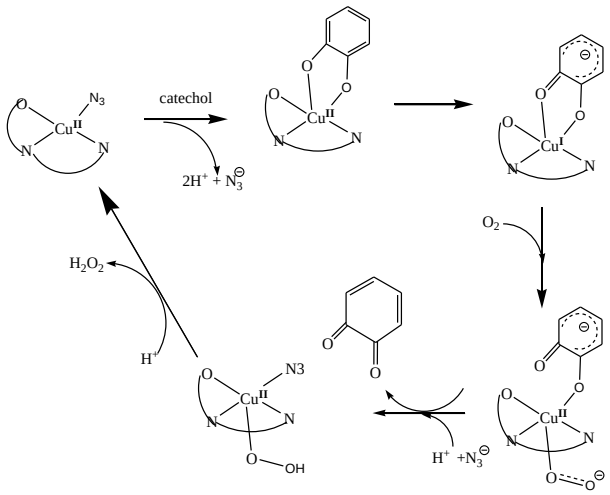

Scheme II: Proposed mechanism of catechol oxidation catalysed by $[Cu(L_1)(N_3)]$(**1**).

A plausible mechanism for the catalysis is given in scheme II. It is suggested that $DTBCH_2$ displaced the N_3^- from the coordination sphere and coordinates as $DTBC^{2-}$ in a bidentate fashion. One electron transfer from $DTBC^{2-}$ converts it to a semiquinone complex having a Cu^{I} core. The Cu^{I} complex rapidly reacts with aerial O_2 to give a Cu^{II}-superoxo complex, containing the semiquinone ligand. Elctron transfer from the semiquionone to superoxide results in dissociation of the quinone and conversion of superoxide to hydroperoxide. This is followed by elimination of H_2O_2 and the catalyst is regenerated.[21,26,79,80] The detection of H_2O_2 from the reaction mixture provides evidence in favour of the proposed mechanism. ESI-MS spectrum (positive ion mode) of a 1:100 mixture of **1** and 3,5-$DTBCH_2$, recorded after 20 min of mixing of the reactants in methanol, shows that apart from the parent complex peak at 300.08, a peak with a m/z value of 543.25 which is consistent with the formula of $[\{Cu(L_1)(3,5\text{-}DTBC^{2-})\}+Na]^+$(**Figure S10** in SI), which thus adds further evidence in favour of the proposed mechanism.

It may be noted that according to the mechanism proposed in scheme II, the Cu(II) complex must have a square planar geometry with a labile ligand in the square plane, for it to be catalytically active. This may be the reason why complex **2**, having a chain like structure with 4+1 coordination of the Cu(II) center is inactive as a catalyst. Comparing the catalytic efficiency of complex **1** with a very similar complex [Cu(L)Cl] (L = $^-$O,N,N-donor Schiff base formed by condensation of pyridoxal and 2-aminomethyl pyridine),[26] one observes that [Cu(L)Cl] is ~10^3 times more catalytically efficient than complex **1**. The much lower Cu(II)/Cu(I) potential (−0.28 V) of [Cu(L)Cl] compared to **1** (−0.55 V), as well as the relatively weaker Cu-Cl bond in the former complex compared to much stronger Cu-N_3 bond in **1** (dCu-N(Azide) = 1.959 (2)Å in **1**, d(Cu-Cl) = 2.288(1) Å in [Cu(L)Cl]] may account for this large difference in their catalytic efficiencies.

3.9 DFT calculation results

DFT calculations were performed on the complexes and the frontier orbitals of **1** are depicted in **Figure 9** and while those of **2** are shown in **Figure S11** in Supplementary material. For complex **1** the SOMO (α-HOMO) has only 3.17% contribution from Cu while for complex **2** (monomer) the SOMO has only 0.74% Cu contribution. The β-LUMO for complexes **1** and **2** has 48.37% and 53.38% contribution respectively from Cu. However, the unpaired spin density is predominantly centred on the Cu-atom with the contribution of the Cu atom being 48.37% and 51.51% for complexes **1** and **2** respectively (**Figure 10**).

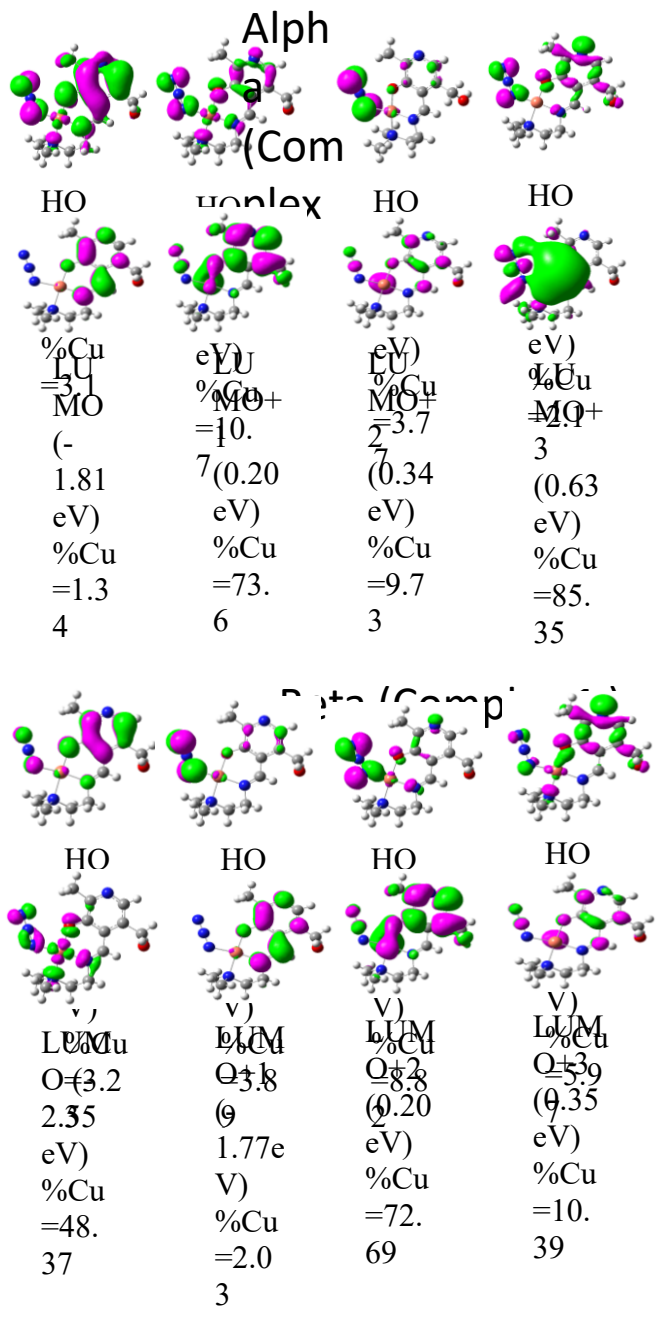

Figure 9 FMOs of complex **1** in gas phase with ISO value cut off 0.04.

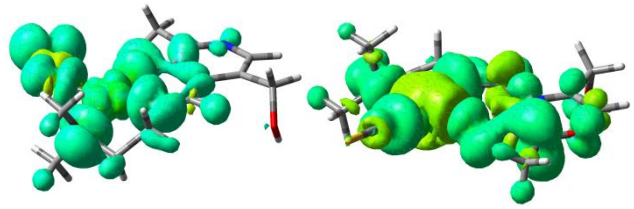

Figure 10 Excess spin density (Alfa) on complexes **1** (left) and **2**(right) with ISO value cut off 0.04.

4. Conclusion.

Cu(II) complexes bearing a pyridoxal appended tridentate Schiff base ligand and azide or thiocyanate coligand are reported in this communication. It is shown that the solid state structures are different in the two complexes, with azide coordinated complex containing monomeric square planar Cu(II), whereas the thiocyanato complex has square pyramidal Cu(II) environment and it exists as a one dimensional chain in the solid state. The two compounds show different reactivity as catalyst for aerial oxidation of catechol (catecholase activity), with complex **1** showing good catalytic efficiency while complex **2** is ineffective as catalyst. The differences in the structures of these two complexes as well as the instability of the Cu(I) species in **2** compared to **1**, as reflected in their electrochemical studies may be the reason for this difference in catalytic activity. Complex **1** shows much stronger DNA-binding ability than complex **2**.

Conflicts of interest

There are no conflicts of interest to declare.

Acknowledgements

SM and BP thank Council of Scientific and Industrial Research (CSIR), New Delhi, MC thanks IIEST, Shibpur and AM thanks DST (W.B.) for research fellowships. SKC acknowledges the All India Council for Technical Education (AICTE) for funding the purchase of a CH1106A potentiostat. SKC thanks Prof. Sabyasachi Sarkar of our institute for allowing using his AOMIX program. We also gratefully acknowledge immense help received from Bruce C. Noll, Bruker AXS, Madison WI, in solving the structure of complex **2**. SAIF, IIT Bombay is acknowledged for recording the epr spectrum.

References

[1] C. Gerdemann, C. Eicken, B. Krebs, *Acc. Chem. Res*., 2002, **35**,183.

[2] S. Itoh, S. Fukuzumi, *Acc. Chem. Res*., 2007, **40**, 592.

[3] E. I. Solomon, M. J. Baldwin, M. D. Lowery, *Chem. Rev.*, 1992, **92**, 521.

[4] E.I. Solomon, U. M. Sundaram, T. E. Machonkiu, *Chem. Rev.*, 1996, **96**, 2563.

[5] Y. Sheng, I. A. Abreu, D. E. Cabelli, M. J. Maroney, M. Teixeira, J. S. Valentine, *Chem. Rev.* 2014, **114**, 3854.

[6] N. G. Rabinett, R. L. Petersen, V. C. Culotta, *J. Biol. Chem.*, 2018, **293**, 4636.

[7] E. I. Solomon, D. E. Heppner, E. M. Johnston, J. W. Ginsbach, J. Cirera, M. Qayyum, M. T. K. Emmons, C. H. Kjaergaard, R. G. Hadt, L. Tian, *Chem. Rev.*, 2014, **114**, 3659.

[8]L. Rulíšek, U. Ryde, *Coord. Chem. Rev.*, 2013, **25**7, 445.

[9] T. Klabunde, C. Eicken, J. C. Sacchettini, B. Krebs, *Nat. Struct. Biol.*, 1998, **5**, 1084.

[10]A. Sánchez-Ferrer, J. N. Rodriguez-Lopez, F. García-Cánovas, F. García-Carmona, *Biochim. Biophys. Acta*, 1995, **1247**, 1.

[11]C. Eicken, B. Krebs, J. C. Sacchettini, *Curr. Opin. Struct. Biol.*, 1999, **9**, 677.
[12] J. N. Hamann, B. Herzigkeit, R. Jurgeleit, F. Tuczek, *Coord. Chem. Rev.,* 2017, **334**, 54.
[13] S. K. Dey, A. Mukherjee, *Coord. Chem. Rev.*, 2016, **310**, 80.
[14] C. J. Cramer, W. Tolman, *Acc. Chem. Res*., 2007, **40**, 601.
[15] N. Kitazima, Y. Moro-oka, *Chem. Rev.*, 1994, **94**, 737.
[16] D. B. Rorabacher, *Chem. Rev.*, 2004, **104**, 651.
[17] L. M. Berreau, S. Mahapatra, J. A. Halfen, R. P. Houser, V. G. Young Jr., W. B. Tolman, *Angew. Chem. Int. Ed.*, 1999, **38**, 207.
[18]S. Dasgupta, I. Mazumder, P. Chakraborty, E. Zangrando, A. Bauza, A. Buzá, A. Frontera, D. Das, *Eur. J. Inorg. Chem.*, 2017, 133.
[19] I. A. Coval, P. Gamez, C. Velle, K. Selmeczi, J. Reedijk, *Chem. Soc. Rev.*, 2006,**35**, 814.
[20] D. Bansal, R. Gupta, *Dalton Trans.*, 2017, **46**, 4617.
[21] P. Chakraborty, J. Adhikary, B. Ghosh, R. Sanyal, S. K. Chattopadhyay, A. Bauzá, A. Frontera, E. Zangrando, D. Das, *Inorg. Chem*., 2014, **53**, 8257.
[22] P. Chakraborty, I. Majumder, H. Kara, S. K. Chattopadhyay, E. Zangrando, D. Das, *Inorg. Chim. Acta*, 2015, **436**, 139.
[23] R. Sanyal, P. Kundu, E. Rychagova, G. Zhigulin, S. Ketkov, B. Ghosh, S. K. Chattopadhyay, E. Zangrando, D. Das, *New. J. Chem.*, 2016, **40**, 6623.
[24] A. K. Ghosh, A. Ali, Y. Singh, C. S. Purohit, R. Ghosh, *Inorg. Chim. Acta*, 2018, **474**, 156.
[25] S. Banerjee, P. Ghorai, P. Brandão, D. Ghsoh, S. Bhuiya, D. Chattopadhyay, S. Das, A. Saha, *New. J. Chem*., 2018, **4**2, 246.
[26] P. Adak, B. Ghosh, A. Bauzá, A. Frontera, A. J. Blake, M. Corbella, C. D. Mukhopadhyay, S. K. Chattopadhyay, *RSC Adv.*, 2016, **6**, 86851.
[27]L. Stryer, Biochemistry, 4th ed., W.H. Freeman and Company, New York, 1995, p. 631.
[28]H. Brurok, J. H. Ardenkjær-Larsen, G. Hansson, S. Skarra,; J. O. G. Karlsson, Laursen, P. Jynge, *Biochem. Biophys. Res. Commun*., 1999, **254**, 768.
[29]A. Aukrust, D. Grace, L. K. Sydnes, K. W. Törnroos, *J. Mol. Struct*., 2002, **641**, 281.
[30] V. M.Leovac, M. D. Joksović, V. Divjaković, L. S. Jovanović, B. Ž. K. Šaranović, A. Pevec, *J. Inorg. Biochem.*, 2007, **101**, 1094.
[31] C. Das, P. Adak, S. Mondal, R. Sekiya, R. Kuroda, S. I. Gorelsky, S. K. Chattopadhyay, *Inorg. Chem*., 2014, **53**, 11426.
[32] P. Talukder, A. Datta, S. Mitra, G. Rosair, M. S. E. Fallah, J. Ribas, *Dalton Trans.*, 2004, 4161
[33]J. Ribas, A. Escuer, M. Monfort, R. Vicente, R. Cortes, L. Lezama, T. Rojo, *Coord. Chem. Rev*., 1999, **193**, 1027.
[34]M. Ohba, H. Okawa, *Coord. Chem. Rev.*, 2000, **198**, 313.
[35]C. Adhikary, S. Koner, *Coord. Chem. Rev*., 2010, **254**, 2933
[36] A. Escuer, R. Vicente, M. A. S. Goher, F. A. Mautner, *J. Chem. Soc. Dalton Trans.*, 1997, 4431.
[37]M. Villanueva, J. L. Mesa, M. K. Urtiaga, R. Cortés, L. Lezama,; M. I. Arriortua, T. Rojo, *Eur. J. Inorg. Chem.*, 2001, 1581.
[38] G.Kickelbick, M. Amirnasr, A. D. Khalaji, S. Dehghanpour, *Aust. J. Chem*., 2003, **56**, 323.
[39] M.Amirnasr, A. D. Khalaji, L. R. Falvello, T. Soler, Polyhedron 2006, **26**, 1967.
[40]A. D. Khalaji, M.Amirnasr, L. R. Falvello, T. Soler, *Anal. Sci.*, 2006, **22**, x47.
[41]Z.-L. You, *Acta Crystallogr*., C61 2005, m297.
[42]P. Nordell, P. Lincoln, *J. Am. Chem. Soc.*, 2005, **127**, 9670.
[43]C. C. Cheng, W. C. H. Fu, K. C. Hung, P. J. Chen, W. J. Wang, Y. T. Chen, *Nucl. Acid Res.*, 2003, **31**, 2227.
[44]A. A. Mokhir, R. Kraemer, *Bioconjugate Chem.*, 2003, **14**, 877.
[45]W. C. Tse, D. L. Boger, *Acc. Chem. Res*., 2004, **37**, 61.
[46]P. Yang, R. Ren, M. L. Guo, A. X. Song, X. L. Meng, C. X. Yuan, Q. H. Zhou, H. L. Chen, Z. H. Xiong, X. L. Gao, *J. Biol. Inorg. Chem.*, 2004, **9**, 495.
[47]A. T. Chaviara, P. J. Cox, K. H. Repana, A. A. Pantazaki, K. T. Papazisis, A. H. Kortsaris, D. A. Kyriakidis, G. S.Nikolov, C. A. Bolos, *J. Inorg. Biochem*., 2005, **99**, 467.
[48] A. M. Pyle, J. P. Rehmann, R. Meshoyrer, C.V. Kumar, N. J. Turro, J. K. Barton, *J. Am. Chem. Soc.*, 1989, **111**, 3051.
[49]S. Satyanarayana, J. C. Dabrowiak, J. B. Chaires, *Biochemistry*, 1992, **31**, 9319.
[50] D. Chatterjee, A. Mitra, G.S. De, *Platinum Met. Rev.*, 2006, **50**, 2.
[51] G.J. Chen, X. Qiao, C.Y. Gao, G.J. Xu, Z.L. Wang, J.L. Tian, J.Y. Xu, W. Gu, X. Liu, S.P. Yan, *J. Inorg. Biochem.*, 2012, **109**, 90.
[52] K. Abdi, H. Hadadzadeh, M. Weil, M. Salimi, *Polyhedron,* 2012, **31**, 638.
[53] H. Khan, A. Badshah, Z. Rehman, M. Said, G. Murtaza, A. Shah, I.S. Butler, S. Ahmed, F.G. Fontaine, *Polyhedron*, 2012, **39**, 1.
[54] R. Indumathy, S. Radhika, M. Kanthimathi, T. Weyhermuller, B.U. Nair, *J. Inorg. Biochem.,* 2007, **101**, 434.
[55]CrysAlisPro, Agilent Technologies, Version 1.171.37.33 (release 27-03-2014 CrysAlis171 .NET)
[56] G. M. Sheldrick, Acta Crystallogr. Sect. A, 2008, **64**, 112.
[57] G. M. Sheldrick, *Acta Cryst. Sect. C,* 2015, **71**, 3.
[58] 'SAINT V8.18C, Bruker AXS Inc., Madison, WI, USA, 2011.
[59] G. M. Sheldrick, TWINABs v2008/4, Bruker AXS Inc., Madison, WI, USA, 2008.
[60]M. E. Reichmann, S. A. Rice, C. A. Thomas, P. Doty, *J. Am. Chem. Soc*., 1954, **76**, 3047.
[61]J. J. Marmur, *Mol. Biol*., 1961, **3**, 208.
[62] G.Cohen, H. Eisenberg, *Biopolymers*, 1969, **8**, 45.
[63] M. J. Frisch, G. W. Trucks, H. B. Schlegel, G. E. Scuseria, M. A. Robb, J. R. Cheeseman, J. A. Montgomery, T. Jr. Vreven, K. N. Kudin, J. C. Burant, J. M. Millam, S. Iyengar, J. Tomasi, V. Barone, B. Mennucci, M. Cossi, G. Scalmani, N. Rega, G. A. Petersson, H. Nakatsuji, M. Hada, M. Ehara, K. Toyota, R. Fukuda, J. Hasegawa, M. Ishida, T. Nakajima, Y. Honda, O. Kitao, H. Nakai, M. Klene, X. Li, J. E. Knox, H. P. Hratchian, J. B. Cross, V. Bakken, C. Adamo, J. Jaramillo, R. Gomperts, R. E. Stratmann, O. Yazyev, A. J. Austin, R. Cammi, C. Pomelli, J. W. Ochterski, P. Y. Ayala, K. Morokuma, G. A. Voth, P. Salvador, J. J. Dannenberg, V. G. Zakrzewski, S. Dapprich, A. D. Daniels, M. C. Strain, O. Farkas, D. K. Malick, A. D. Rabuck, K. Raghavachari, J. B. Foresman, J. V. Ortiz, Q. Cui, A. G. Baboul, S. Clifford, J. Cioslowski, B. B.

Stefanov, G. Liu, A. Liashenko, P. Piskorz, I. Komaromi, R. L. Martin, D. J. Fox, T. Keith, M. A. Al-Laham, C. Y. Peng, A. Nanayakkara, M. Challacombe, P. M. W. Gill, B. Johnson, W. Chen, M. W. Wong, C. Gonzalez, Pople, J. A. *(Revision B.04)*; Gaussian, Inc.: Pittsburgh, PA, **2003**.
[64] D. Becke, *J. Chem. Phys.*, 1993, **98**, 5648.
[65] C. Lee, W. Yang, R. G. Parr, *Phys. Rev. B*, 1988, **37**, 785.
[66] G. A. Petersson, M. A. Al-Laham, *J. Chem. Phys.*, 1991, **94**, 6081.
[67] P. J. Hay, W. R. Wadt, *J. Chem.* Phys., 1985, **82**, 299.
[68] P. J. Hay, W. R. Wadt, *J. Chem. Phys.*, 1985, **82**, 270.
[69]F. A. Maunter, M. A. S. Goher, *Polyhedro*n, 1996, **15**, 5.
[70]F. A. Maunter, M. A. S. Goher, *Polyhedron*, 1993, **12**, 2823.
[71]K. R. Reddy, M. V. Rajasekharan, J.-P. Tuchagues, *Inorg. Chem.*, 1998, **37**, 5978.
[72]A. B. P. Lever, Inorganic Electronic Spectroscopy, second ed., Elsevier Science, New York, 1984.
[73]X. W. Liu, J. Li, H. Li, K. C. Zheng, H. Chao, L.N. Ji, *J. Inorg. Biochem*., 2005, **99**, 2372.
[74]F. J. Meyer-Almes, D. Porschke, *Biochemistry*, 1993, **32**, 4246.
[75]G. M. Howe, K. C. Wu, W. R. Bauer, *Biochemistr*y, 1976, **19**, 339.
[76]R. S. Kumar, S. Arunachalam, V. S. Periasamy, C. P. Preethy, A. Riyasdeen, M. A Akbarsha, *J. Inorg. Biochem.*, 2009, **103**, 117.
[77]S. Tabassum, S. arveen, F. Arjmand, *Acta Biomater.*, 2005, **1**, 677.
[78]M. Lee, A. L. Rhodes, M. D. Wyatt, S. Forrow, J. A. Hartley, *Biochemistry*, 1993, **32**, 4237.
[79] A.Biswas, K. L. Das, M. G. B. Drew, C. Diaz, A. Ghosh, *Inorg. Chem.*, 2012, **51**, 10111.
[80]J. Kaizer, T. Csay, G. Speier, M. Giorgi, *J. Mol. Catal. A: Chem.*, 2010, **329**, 71.

